Charge-state distributions of nitrogen ions resulting from the foil-induced dissociation of 4.2-MeV N_2^+ ions

D. Maor,* P. J. Cooney,† A. Faibis, E. P. Kanter, W. Koenig, and B. J. Zabransky
Physics Division, Argonne National Laboratory, Argonne, Illinois 60439
(Received 20 March 1985)

We have studied the dependence of the charge-state distributions of heavy-ion fragments resulting from the foil-induced dissociation of 4.2-MeV N_2^+ ions on the thickness of the carbon target foil. The results are compared to those distributions measured for impact of 2.1-MeV N^+ projectiles. Whereas the mean charge state for atomic-ion impact is already equilibrated in moderately thin targets (2 $\mu g/cm^2$), those measured for molecular-ion impact are strongly dependent on the target thickness, even for the thickest targets (20 $\mu g/cm^2$). The distributions for molecular-ion impact show a marked shift towards lower charge states, evidencing an enhanced electron-capture probability over the case of monatomic-ion impact. A quantitative model is described which explains this phenomenon by reducing the two-center potential of the cluster fragments to a separation-dependent one-center potential.

I. INTRODUCTION

When diatomic projectiles are incident at MeV energies upon a foil, most of the binding electrons of the projectile molecule are stripped off within the first few angstrom units of penetration into the solid target. The resulting two highly charged nuclei rapidly separate due to their mutual Coulomb repulsion, converting their initial electrostatic potential energy into kinetic energy of their relative motion. This dissociation process (which proceeds with a characteristic time of several femtoseconds) has been termed a Coulomb explosion.[1] For fast (MeV) ions in thin (~ 100 Å) foils, the constituent nuclei traverse the target in ~ 1 femtosecond. These Coulomb explosion fragment ions then emerge into the vacuum downstream of the target with an internuclear separation ~ 1—5 Å. Because of this fact, fast molecular-ion beams provide a unique source of energetic projectile nuclei which are correlated both spatially and temporally. The recognition of this feature has prompted several recent investigations of various aspects of the interactions of these ions with matter.[2] In particular, the foil-induced dissociation of fast molecular ions has been used by several groups to provide new information about molecular-ion structures,[3,4] the charge states of fast ions inside and outside solids,[5,6] the interactions of such ions with the solid,[2,7,8] as well as other atomic collision phenomena.

Because of the proximity of the ions during, and immediately after, traversal of the target, Coulomb explosion experiments provide a way to study the evolution of final charge states of heavy ions with a femtosecond time scale.[5] Already, several experimenters have reported charge-state-dependent effects seen with molecular-ion clusters.[5,6,9–11] For short dwell times in the target (so that the fragment ions are close upon exit) experiments with hydrogen molecular ions have shown an enhancement of the yield of neutral hydrogen fragments from the Coulomb explosion.[12] It has been argued that this is a consequence of the enhanced density of electrons at the exit produced by the correlated pair of ions. This phenomenon has been shown to be a function of the relative orientation of the exiting ions.[9]

There have also been suggestions of enhanced electron capture from experiments with diatomic clusters of heavy ions.[11,10,13] These results have taken the form of fragment charge-state distributions which appear to be shifted toward lower charge states in comparison to those measured with isotachic-monatomic-ion beams. These results, while highly suggestive, have not been convincing because of the effect of the broadening of the angular distributions of the emitted fragment ions due to the Coulomb explosion. Because this broadening increases with increasing charge state, experiments which do not fully integrate over all fragment ions are susceptible to systematic errors which *lower* the observed mean charge state.[13] While providing a utilitarian mean charge state, the results to date have made it difficult to properly interpret the observed differences between mean charges observed with molecular- and atomic-ion beams and thus there have been no theoretical attempts to explain these data. We report the results of an experiment designed to address these shortcomings. These findings have enabled us to form a simple model explaining the observed phenomena.

II. EXPERIMENT

Data for this experiment were collected at Argonne National Laboratory's 4.5 MV Dynamitron accelerator, using a beam line specifically designed to measure, with very high resolution, the distribution in energy and in angle of ions resulting from the dissociation of MeV-molecular ions. The general characteristics of this beam line have been described in greater detail elsewhere,[14] so only features of the apparatus pertinent to the present experiment will be emphasized here.

Isotachic beams of 2.1-MeV N^+ and 4.2-MeV N_2^+

were individually extracted from the accelerator, magnetically analyzed, and collimated to an angular divergence of 0.11 mrad full width at half maximum (FWHM) by a pair of 1-mm-diam apertures separated by 7.7 m. Such long flight paths can produce up to a few percent of undesired particles in the incident beam as a result of charge-changing and fragmenting collisions with residual gas molecules, even with the vacuum of about 2×10^{-7} Torr maintained in the beam line. To solve this problem, the incident beam passes through a uniform electric field just ahead of the target foils. The resulting "predeflection" of the incident beam separates the desired ions from any unwanted ones. The flux of ions incident on the target was monitored by "chopping" the incident beam and counting the number of ions scattered from the gold surface of the chopper blades.

The targets used in these experiments were a set of five thin, amorphous, self-supporting carbon foils, ranging in thickness from 75—780 Å. These thicknesses were chosen to provide dwell times of the incident ions inside the target ranging from 1.4—14.5 femtoseconds. In the case of incident N_2^+, this translates into a range of internuclear separations of 1.5—9 Å for the two resulting fragment ions at the exit side of the foil. The thickness of the targets was monitored during the experiment by repeated measurements of the energy loss of the incident N^+ in each target relative to the energy of the incident ions passing through the "pinholes" in our thinnest targets.[14]

The outgoing ions were detected 6.3 m downstream of the target by an electrostatic analyzer having a fractional energy resolution $\Delta E/E=8.4\times10^{-4}$ (FWHM) and an overall angular resolution of 0.17 mrad (FWHM). Since this analyzer is in a fixed location, angular distributions of the outgoing fragments are obtained by stepping a voltage applied to a set of parallel-plate deflectors, located just downstream of the targets. The resulting "postdeflection," used together with the "predeflection" already discussed, also serves to separate the angular distributions of the variously charged nitrogen ions leaving the target. This, together with the charge-state selectivity of the electrostatic analyzer, allows the measurement of angular distributions for each final charge state with assurance that only the selected charge state is being detected. Energy spectra of the outgoing ions were obtained by setting the postdeflection voltage to a value corresponding to the peak yield for a particular charge state and then stepping the voltage applied to the analyzer.

III. RESULTS AND ANALYSIS

Figures 1 and 2 display examples of sets of energy and angular distributions measured for a carbon target 2 $\mu g/cm^2$ thick for molecular and atomic projectiles, respectively. Before these data can be used to extract charge-state distributions, the effects of contaminant beams must be removed. This problem arises mainly for the molecular projectiles, which are accompanied by a small fraction of N^+ and N^0 from molecules dissociated upstream of the target in collisions with residual gas molecules. As explained in Sec. II, the pre- and postdeflection of the beam on both sides of the target will

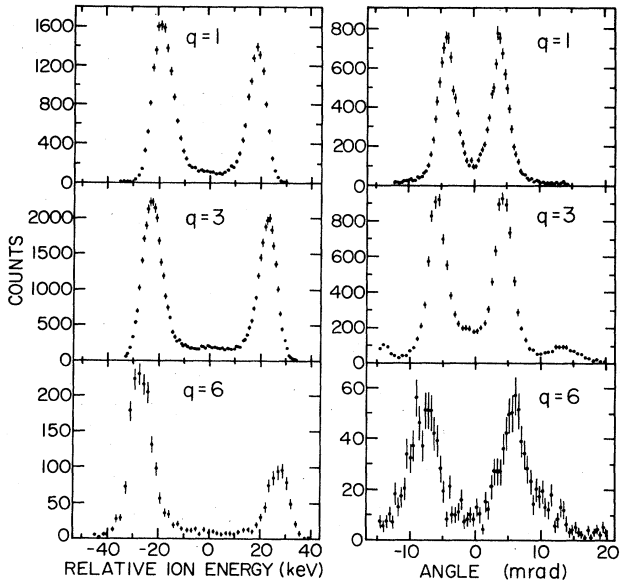

FIG. 1. Some representative energy and angular distributions for nitrogen fragment ions, in various final charge states q, resulting from the dissociation of 4.2-MeV N_2^+ in a 2-$\mu g/cm^2$ carbon foil. The laboratory energies are expressed relative to the mean energy of the exciting ions in each case.

move the exiting ions resulting from these isotachic contaminants to somewhat different angles in the angular spectra. Indeed, they can be seen in some of the angular scans in Fig. 1 as small peaks on the flanks of the main distribution (especially evident for $q=3$). Owing to their well-determined shape and relatively small size, they can

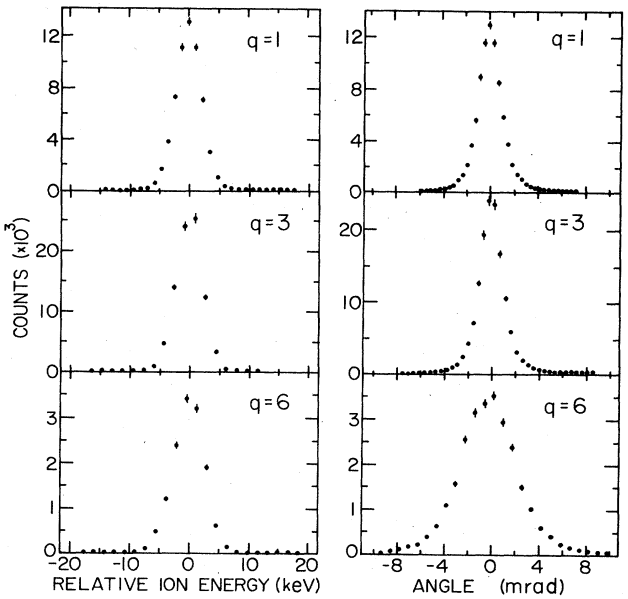

FIG. 2. As in Fig. 1 for the case of impact by 2.1-MeV N^+ ions.

be subtracted from the main distribution with good accuracy (see discussion of errors below).

Now the abundance fraction of each exiting charge state (from 1 + to 6 +) has to be extracted from the measured energy and angular distributions. The analysis is done differently for the molecular and atomic projectiles, as explained below.

In the molecular case, the velocity with which the fragment arrives at the detector is given by $\mathbf{V}=\mathbf{u}+\mathbf{V}_0$, where $\mathbf{V}_0$ is the beam velocity and $\mathbf{u}$ is the additional velocity acquired by the fragment due to the Coulomb explosion. Multiple scattering, initial vibrational excitation of the molecule, etc., will cause $\mathbf{u}$ to have a distribution in magnitude as well as its obvious distribution in spatial orientations, thus yielding the characteristic distributions both in the energy and angular scans (see Fig. 1). Since $|\mathbf{V}_0|/|\mathbf{u}| \sim 100$, the angular deviation from the center at the average energy is approximately proportional to $|\mathbf{u}|$. Because the internuclear vectors in the incident molecules are randomly oriented in space, we expect an isotropic distribution of $\mathbf{u}$, every pair of points equidistant from the center of the angular scan representing the intensity on a spherical shell in the $\mathbf{u}$ distribution. The total number of molecular fragments emerging with the charge state q [$Y_M(q)$] will therefore be proportional to

$$Y_M(q) \approx \int N_M(\theta,q)\theta^2 d\theta \tag{1}$$

where $N_M(\theta,q)$ is the number of counts at laboratory angle θ (measured with respect to the beam direction). The assumption of isotropy is certainly not true near the beam direction, where the asymmetry due to wake effects appears[7] (see Fig. 1). However, this effect is present for only a very small fraction of the total solid angle and is not liable to affect the fragment angular distributions for incident molecules with internuclear vectors transverse to the beam direction.[15] Apart from this negligible effect, measurements of full "rings" show that the $\mathbf{u}$ distributions are generally isotropic (see, e.g., Ref. 15).

In the case of atomic impact, the distributions in energy and angle of the exiting ions are principally determined by energy straggling and small-angle multiple scattering processes in the target. The latter effect especially can vary considerably with charge state.[16] Figure 2 displays such spectra for impact by atomic projectiles. Since the angular scan is taken at the average energy, with a fixed energy width, the ratio of the total counts in the energy scan to the peak value is first determined

$$R = \int N(E)dE/N(E_0) . \tag{2}$$

Then, each point in the angular scan is given a weight θ since it represents a ring of all particles scattered to that particular angle, at energy E_0. The normalization to the whole energy spectrum is then done by multiplication by R. This results in

$$Y_A(q) \approx R \int N_A(\theta,q)\theta\, d\theta . \tag{3}$$

When the yields of the different charge states have been normalized by means of the counts in the detector at the chopper, the charge-state distribution is readily extracted. Uncertainties in the results have two principal origins: statistics and the subtraction of the contaminants. In the present experiment, the statistical errors were low and thus the second factor is dominant. The estimated uncertainties are $\pm 1.5\%$ for the most probable charge states ($q=2-4$). For the remaining charge states, errors were (3—5)%, principally due to the background subtraction procedure and to the lower yields. The error in the average charge state is, of course, smaller—generally about $\pm 0.7\%$ ($\sim \pm 0.02$ units of charge). The corresponding charge fractions [$F_A(q)$ and $F_M(q)$] are derived by normalizing the yields $Y_A(q)$ and $Y_M(q)$, respectively. Figure 3 displays some typical charge-state distributions of the exiting fragments both for atomic and molecular projectiles for 100- and 345-Å targets.

In Fig. 4 the average charge states for the molecular and atomic projectiles, $\bar{q}_M$ and $\bar{q}_A$, are shown as functions of the target thickness. The prominent feature in these figures is the fact that while the atomic distribution seems to be already equilibrated at about 100 Å, the molecular distribution starts out with an average charge state smaller by about 0.25 charge units than the atomic one, and approaches it slowly, not quite reaching there even for the thickest target used. This represents a shift of $\sim 8\%$ in the mean charge state. The slight decrease in the average charge state for the thickest target in the atomic case is due to the fact that the distributions were measured for a constant incoming rather than a constant exit velocity. For the thickest target the projectile suffers an already non-negligible energy loss of 128 keV, which should reduce the average charge state by 0.07 of a charge unit.[17] This number agrees very well with the decrease seen in Fig. 4 (see dashed lines). For the molecular case, this effect is obscured by the still increasing $\bar{q}_M$ toward $\bar{q}_A$ as mentioned above.

The same features are again demonstrated in Fig. 5,

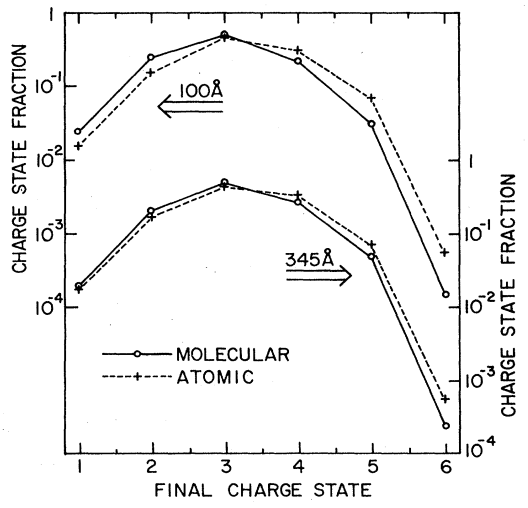

FIG. 3. Normalized charge-state distributions [$F_M(q)$ and $F_A(q)$] for nitrogen ions in various final charge states resulting from impact of 2.1-MeV/atom N_2^+ and N^+ ions, respectively. Data are shown for 100- and 345-Å-thick targets. The lines are drawn merely to guide the eye.

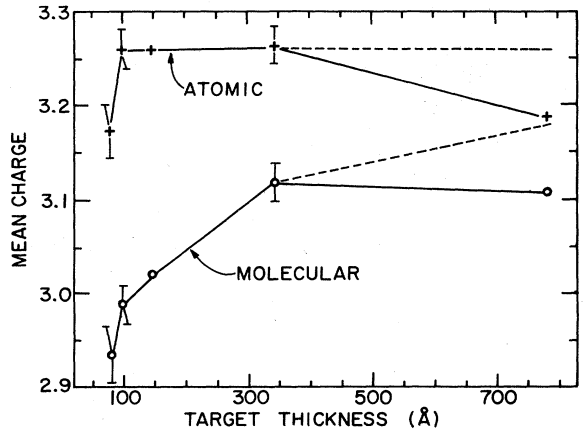

FIG. 4. Mean final charge states, deduced from the measured charge-state distributions, as a function of the target thickness. Data are shown for both the cases of atomic- and molecular-ion impact. Lines are drawn to guide the eye. The dashed lines include the correction, as described in the text, for the energy loss in the target.

where the ratios of the fractions from molecular projectiles to those for atomic projectiles are displayed for each measured charge state, as a function of target thickness. Another interesting feature of the data, which is most prominent in Fig. 5, concerns the very large difference between the atomic and molecular projectiles for the exiting $6+$ charge state. Whereas for $1+$ to $5+$ the ratios of the exiting charge fractions $F_A(q)/F_M(q)$ start out in the range 0.6—1.4 for the thinnest target and get quite close to unity for the thickest one, $F_A(6)/F_M(6)\simeq 5$ for the thinnest target and targets much thicker than the ones measured are needed to bring it close to unity. It should be pointed out that owing to its very small absolute value, changes in the $6+$ fraction do not affect the average charge state appreciably.

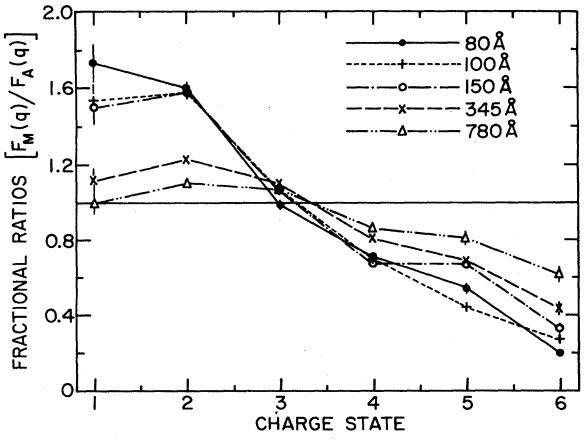

FIG. 5. Ratios of the charge-state fractions for molecular- and atomic-ion impact as a function of the final exit-ion charge state for varying target thicknesses as shown.

IV. DISCUSSION

The main features of the data presented above are the following:

(i) For the case of molecular-ion impact, there is a total *shift* of the charge-state distributions toward lower charges when compared to those distributions measured for atomic-ion impact. For the dominant charge states, the *shapes* of the distributions are not significantly different for atomic- and molecular-ion impact.

(ii) Although for atomic-ion impact the yields of the dominant charge states are equilibrated in the thinnest targets, the case of molecular-ion impact shows apparent nonequilibration even for the thickest targets, though the trend is to asymptotically approach the atomic distribution with increasing target dwell time.

The first observation underscores the fact that this phenomenon cannot result from the redistribution of valence electrons between the dissociation fragments exiting the foil. Because it conserves valence electrons, such a process would not produce a shift in the mean charge, but would instead merely narrow the distribution. The shift must be caused by an enhanced capture of target electrons. Redistribution effects no doubt do play a role in suppressing the yields of the very rare highly charged ions far from the equilibrium mean (i.e., $6+$ and $7+$), and therefore probably account for the anomalous behavior of the $6+$ fraction noted above. Because of the low yields of such ions, this should not significantly affect the yields of the predominant charge states near the mean. The second result implies that the cross sections for capture and loss of target electrons are dependent on the internuclear separation of the dissociation fragments. We thus hypothesize that in both cases, the absolute magnitudes of the charge-exchange cross sections, for the exiting ions, are sufficiently large to achieve equilibrium in all of the targets. However, for the case of the molecular projectiles, the cross sections for electron capture at exit are dependent upon the internuclear separation and thus lead to apparent nonequilibration (i.e. target-thickness dependence) of the measured charge-state distributions.

In order to pursue this question further, we have sought to extract "effective" capture and loss cross sections for both the cases of atomic- and molecular-ion impact. Although these distributions are equilibrated, it is simple to extract the ratios of capture and loss cross sections for single-electron charge-changing, if multiple-electron processes can be neglected.[18–21] Studies of ion-atom collisions involving nitrogen ions in this velocity range support such an assumption as multiple charge-changing cross sections are found to be at least an order of magnitude smaller than those for the corresponding single-electron processes.[18,22–23] Furthermore, the symmetry of our measured charge-state distributions is a strong indication that multiple electron processes do not play an important role in the formation of the charge states we have detected.[20] Subject to this assumption, for a finite set of ion charge states at equilibrium, single-electron loss and capture must cancel and thus[18]

$$F(q)\sigma_l^q = F(q+1)\sigma_c^{q+1} \tag{4}$$

where σ_l^q and σ_c^q are the effective single-electron charge-changing cross sections for loss and capture respectively, by an ion with initial charge state q.

In order to reduce the number of free parameters required to describe the equilibrium charge-state distributions, we now impose two additional simplifying assumptions on the charge-state dependencies of these cross sections:

(i) The capture cross sections σ_c^q are assumed to be proportional to an unknown power (p) of the charge state q, i.e.,

$$\sigma_c^q = C\sigma_0 q^p \ . \tag{5}$$

(ii) The loss cross sections σ_l^q are assumed to be proportional to the number of L-shell electrons for each charge state, i.e.,

$$\sigma_l^q = \sigma_0(5-q) \tag{6}$$

where C and σ_0 are constants of proportionality.

Both of these assumptions are based on the fact that for the ion beams studied in this work, the K-vacancy fractions are small, as is evident from the 6+ and 7+ fractions in the measured charge-state distributions, and thus we are concerned primarily with L-shell electrons. Under such conditions, the single-electron-capture cross sections do indeed exhibit a power-law dependence upon q, with exponents varying between ~ 2 and ~ 5, depending upon the collision partners and ion velocities for the cases studied.[20–25] Also under these conditions, the total loss cross section for electrons within a given electronic shell, is expected to be proportional to the number of such equivalent electrons.[18] This is the basis for our second assumption.

Using these assumptions, and Eq. (4), we are able to extract the power p and constant C by best fitting the data. The results of this fitting procedure are displayed in Fig. 6. The value of the power p extracted (2.8 ± 0.3) is consistent with the expected range noted above. The constant

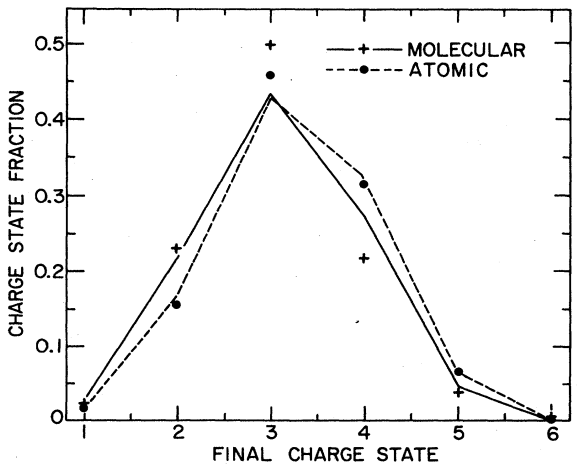

FIG. 6. Emergent-ion charge-state fractions for atomic- and molecular-ion impact upon a 345-Å target, as in Fig. 3, plotted with a linear scale. The dashed and solid lines are fits to the atomic and molecular data, respectively, as described in the text.

C was determined by this fitting procedure to be 0.05 ± 0.02. It is interesting to note in this context that subject to the assumptions stated above, the generalized Oppenheimer-Brinkmann-Kramers formula[20] (OBK) would predict that the capture cross section exhibit a charge-state dependence scaling roughly as $q^2(q+3)$. A least-squares fit of a power-law dependence to the capture cross sections calculated with the OBK formula, as has been done with the experimental data, gives an exponent of 2.5. Using the capture cross sections given by this formula, and loss cross sections derived from scaled ionization data,[26] the constant C is predicted to be 0.06. Based on these comparisons, we believe that these cross sections accurately represent the data for the case of impact by atomic ions.

In order to describe the case of impact by molecular ions, we note that the target thickness required to equilibrate the charge-changing processes, is much thinner than 2 μg/cm^2, as evidenced by the data for atomic-ion impact. Indeed, using the capture and loss cross sections calculated as described above, we find a predicted equilibrium length of 0.2 μg/cm^2. We thus assume that the capture and loss cross sections for the case of molecular-ion impact are also sufficiently large to equilibrate the charge-changing processes within the thicknesses of targets studied. However, the electron-capture cross sections in this case are presumed to be dependent upon the internuclear separation of the exiting fragments and thus implicitly thickness dependent. Because of the short equilibration length, it suffices to calculate these cross sections at the exit of the foil. Upon exit from the foil, the clusters studied in these experiments have mean internuclear separations varying from 1.2 to nearly 9 Å, calculated on the basis of a simple Coulomb explosion in the foil. These distances are large compared to the L-shell radius of the atomic-nitrogen fragment ions (~ 0.4 Å) and the adiabatic distance (0.41 Å) for projectile ionization.[27] Based on these considerations, we approximate the two-center potential of the exiting cluster as an effective central potential in which the partner fragment of each exiting ion produces a weak perturbation of the atomic potential of that ion. We thus assume, for the purpose of computing the capture cross section, an effective charge q^{eff} given by

$$q^{\text{eff}} = q + x\langle q \rangle \tag{7}$$

where, $\langle q \rangle$ is the measured mean exit charge and x is a perturbation parameter to be determined. The parameter x will, of course, be thickness dependent, asymptotically approaching zero as the target thickness (and exit separations of the fragments) increases.

Substituting q^{eff} for q in Eq. (5), and using the constants p and C obtained from fitting the atomic data, we use Eqs. (4)–(6), with x as the only free-fitting parameter, to fit the molecular charge-state distributions for each target thickness. A typical fit is shown in Fig. 6. The parameters x extracted by this procedure are displayed in Fig. 7 as a function of the mean exit separation of the exiting fragments. It is interesting to ascribe a physical interpretation to this parameter by noting that for internuclear separations (R_{ex}) large compared to the L-shell ra-

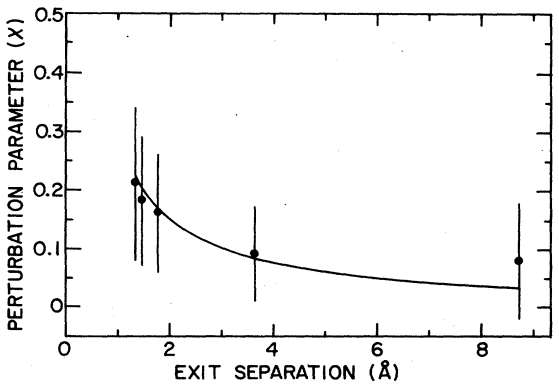

FIG. 7. The perturbation parameter x as a function of the internuclear separation of the nitrogen cluster fragments upon exiting the target foil (R_{ex}). This parameter is obtained by fitting the charge-state distributions, for the case of impact by 4.2-MeV N_2^+ ions on targets of various thicknesses, as described in the text. The solid line is a plot of the ratio r_L/R_{ex}.

dius (r_L) we may rewrite the two-center potential acting on an electron at r_L as

$$q/r_L+\langle q\rangle/R_{ex}=[q+(r_L/R_{ex})\langle q\rangle]/r_L \ . \quad (8)$$

We thus expect an enhancement in the effective charge as postulated by Eq. (7) and identify x as the ratio r_L/R_{ex}. This ratio, which is plotted as a solid line in Fig. 7, shows remarkably good agreement with both the absolute magnitude and the trend of the data with increasing target thickness.

V. CONCLUSIONS

We have conclusively demonstrated the systematic shift of the distributions of final charge states, for Coulomb explosion fragments compared to isotachic-monatomic-ion beams. This shift includes both an enhanced yield of lower charge states (below the equilibrium mean) concomitant with a decrease in the yield of charge states above the mean and thus essentially preserves the shapes of the distributions. From the trends of the data, it was shown that this shift is attributable to an enhanced electron-capture probability for ions emerging from the target foil as spatially correlated diatomic clusters.

A simple model was presented relating the charge-state distributions measured for molecular-ion impact to the equilibrium distribution measured for the case of impact by a monatomic-ion beam. This model describes the apparent nonequilibration of the molecular-ion charge-state distributions as a simple consequence of electron-capture cross sections dependent upon the internuclear separations of the exiting cluster fragments. Because this separation is large compared to the orbital radius of captured electrons, the enhancement of the electron-capture cross sections can be treated as a weak perturbation of the potential at the position of the electron. Such an approximation allows the estimation of this enhancement. This model, though admittedly overly simplified, resolves the long-standing problem of understanding the distributions of final charge states when heavy diatomic molecular ions exit from solids.

ACKNOWLEDGMENTS

The authors wish to thank Professor T. J. Gray for his helpful comments on this work. One of us (D.M.) would like to express his gratitude to the Physics Division at Argonne National Laboratory for hospitality and support while this research was being performed. This work was supported by the U.S. Department of Energy (Office of Basic Energy Sciences), under Contract No. W-31-109-Eng-38.

*Permanent address: Department of Physics, The Technion—Israel Institute of Technology, Haifa 32000, Israel.
†Permanent address: Department of Physics, Millersville University, Millersville, PA 17551.

[1]See, e.g., J. Remillieux, Nucl. Instrum. Methods **170**, 31 (1980); D. S. Gemmell, *ibid.* **170**, 41 (1980); R. Laubert, IEEE Trans. Nucl. Sci. **NS-26**, 1020 (1979).
[2]E. P. Kanter, Comments At. Mol. Phys. **11**, 63 (1981).
[3]D. S. Gemmell, Chem. Rev. **80**, 301 (1980).
[4]E. P. Kanter, in *Molecular Ions*, edited by J. Berkowitz and K.-O. Groeneveld (Plenum, New York, 1983), p. 463.
[5]I. Plesser, E. P. Kanter, and Z. Vager, Phys. Rev. A **29**, 1103 (1984).
[6]A. Breskin, A. Faibis, G. Goldring, M. Hass, R. Kaim, Z. Vager, and N. Zwang, Phys. Rev. Lett. **42**, 369 (1979).
[7]Z. Vager and D. S. Gemmell, Phys. Rev. Lett. **37**, 1352 (1976).
[8]M. F. Steuer, D. S. Gemmell, E. P. Kanter, E. A. Johnson, and B. J. Zabransky, Nucl. Instrum. Methods **194**, 277 (1982).
[9]P. J. Cooney, D. S. Gemmell, E. P. Kanter, W. J. Pietsch, and B. J. Zabransky, Nucl. Instrum. Methods **170**, 73 (1980).
[10]P. Thieberger, in Proceedings of the Workshop on Physics with Fast Molecular-Ion Beams, Argonne, 1979, edited by D. S. Gemmell [Argonne National Laboratory Report No. ANL/PHY-79-3, 1979 (unpublished)], p. 41.
[11]W. S. Bickel, Phys. Rev. A **12**, 1801 (1975).
[12]M. J. Gaillard, J.-C. Poizat, A. J. Ratkowski, J. Remillieux, and M. Auzas, Phys. Rev. A **16**, 2323 (1977).
[13]Ch. Stoller, M. Suter, R. Himmel, G. Bonani, M. Nessi and W. Wolfli, IEEE Trans. Nucl. Sci. **NS-30**, 1074 (1983).
[14]B. J. Zabransky, P. J. Cooney, D. S. Gemmell, E. P. Kanter, and Z. Vager, Rev. Sci. Instrum. **54**, 531 (1983).
[15]E. P. Kanter, P. J. Cooney, D. S. Gemmell, K.-O. Groeneveld, W. J. Pietsch, A. J. Ratkowski, Z. Vager, and B. J. Zabransky, Phys. Rev. A **20**, 834 (1979).
[16]E. P. Kanter, Phys. Rev. A **28**, 1401 (1983).
[17]Y. Baudinet-Robinet, Phys. Rev. A **26**, 62 (1982).
[18]V. S. Nikolaev, Usp. Fiz. Nauk **85**, 679 (1965) [Sov. Phys. Usp. **8**, 269 (1965)].
[19]H.-D. Betz, Rev. Mod. Phys. **44**, 465 (1972).
[20]H.-D. Betz, in *Methods of Experimental Physics*, edited by P.

Richard (Academic, New York, 1980), Vol. 17, p. 73.
[21]H.-D. Betz in *Applied Atomic Collision Physics: Condensed Matter,* edited by H. S. W. Massey *et al.* (Academic, New York, 1983).
[22]H. H. Lo and W. L. Fite, At. Data **1**, 305 (1970).
[23]J. R. MacDonald and F. W. Martin, Phys. Rev. A **4**, 1965 (1971).
[24]V. S. Nikolaev, L. N. Fateeva, I. S. Dmitriev, and Ya. A. Teplova, Zh. Eksp. Teor. Fiz. **33**, 306 (1957) [Sov. Phys.—JETP **6**, 239 (1957)].
[25]H.-D. Betz, G. Ryding, and A. B. Wittkower, Phys. Rev. A **3**, 197 (1971).
[26]J. D. Garcia, R. J. Fortner, T. M. Kavanagh, Rev. Mod. Phys. **45**, 111 (1973).
[27]J. Bang and J. M. Hansteen, Mat.-Fys. Medd. K. Dan. Vidensk. Selsk. **31**, No. 13 (1959).